INTERNATIONAL SOCIETY FOR
SOIL MECHANICS AND
GEOTECHNICAL ENGINEERING

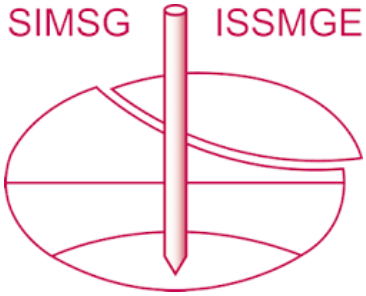


*This paper was downloaded from the Online Library of the International Society for Soil Mechanics and Geotechnical Engineering (ISSMGE). The library is available here:*

*https://www.issmge.org/publications/online-library*

*This is an open-access database that archives thousands of papers published under the Auspices of the ISSMGE and maintained by the Innovation and Development Committee of ISSMGE.*

*The paper was published in the proceedings of the 7th International Conference on Earthquake Geotechnical Engineering and was edited by Francesco Silvestri, Nicola Moraci and Susanna Antonielli. The conference was held in Rome, Italy, 17 – 20 June 2019.*

*Earthquake Geotechnical Engineering for Protection and Development of Environment and Constructions – Silvestri & Moraci (Eds)*
*© 2019 Associazione Geotecnica Italiana, Rome, Italy, ISBN 978-0-367-14328-2*

# Long term cyclic behavior and strength of marine silty sand investigated by cyclic direct simple shear apparatus

J.M. Kim, S.W. Son, J.C. Yoon, P. Bagheri, D.H. Lee & S.H. Sim
*Pusan National University, Busan, Korea*

ABSTRACT: As a renewable clean source of energy, offshore wind power is capable of supplying increasingly demand for energy. Offshore structures are normally subjected to various cyclic loads from wind, waves, and tidal loads. Depending on the cyclic degradation, the foundation load capacity under cyclic loading conditions may be different than the monotonic loading conditions. Hence, special attention should be given to evaluate the effect of cyclic load on the behavior of soil and structure. In this study, utilizing Cyclic Direct Simple Shear apparatus (CDSS), the long-term cyclic behavior of marine silty sand is investigated. Failure contours are proposed using the test results. The failure contours are useful tool to predict the shear behavior of the ground when subjected to the dynamic loading. The failure contours are generated considering various parameters including confining pressure and soil relative density. Finally, the effect of vertical loading on the failure contours are investigated.

## 1 INTRODUCTION

Burning fossil fuels is the main cause for the global warming and is harmful for the environment and public health. Therefore, it is necessary to develop eco-friendly and clean energy resources. Wind energy is a renewable energy that is sustainable and will never run out. In recent years, the installation of offshore wind farms to produce efficient energy are increasing. Marine ground is subjected to cyclic loads such as ripples and wind loads for a long period of time. Andersen et al. 1999 evaluated the behavior of the structure foundation soil subjected to cyclic loading by performing laboratory dynamic test, and found that the average and cyclic shear stress, drainage condition, and stress path affect the number of cyclic loading and failure behavior that reach failure. Andersen 2009 assessed the behavior of clayey, silty and sandy soils subjected to the dynamic shear stress and cyclic loading, and proposed the design graph. Ryu et al. 2015 and Ko et al. 2017 presented failure contours with stress-based failure criterion for undrained failure behavior of Marine silty sand subjected to cyclic loading under different relative soil densities. Son et al. 2017 proposed 3D failure contours and failure contours according to various relative densities that can be used in the design procedure. In this study, the behavior of marine ground under cyclic loading was evaluated. The effects of confining pressure were also investigated.

## 2 FAILURE BEHAVIOR OF SOIL

### 2.1 *Failure behavior*

Andersen et al. 1988 reported that the design graph is expressed as a graph about the cyclic stress ratio (CSR) and the average stress ratio (ASR) to the shear strain and the number of cyclic loading at the time of reaching failure. The cyclic shear stress ratio and the average stress ratio are defined by equation (1). Where, $\tau_{cy}$ is cyclic shear stress, $\tau_a$ is average shear stress, and $\sigma_{vc}'$ is vertical confining pressure.

$$CSR = \frac{\tau_{cy}}{\sigma_{vc}'}, ASR = \frac{\tau_a}{\sigma_{vc}'} \quad (1)$$

Figure 1 (a) shows changes of the cyclic and average shear stress, pore water pressure, and shear strain by cyclic loading. As cyclic loading is applied to the specimen under the undrained conditions, a pore water pressure develops, and an increase of pore water pressure causes permanent shear strain ($\gamma_p$) and cyclic shear strain ($\gamma_{cy}$), Andersen 2009. Figure 1 (b) shows the behavior of stress-strain by cyclic loading. Cyclic shear stress ($\tau_{cy}$) generates cyclic shear strain ($\gamma_{cy}$), and average shear stress ($\tau_a$) generates permanent shear strain ($\gamma_p$). Average and cyclic shear stresses are also defined as the stresses in the in-situ soil condition and the weight of the structure, respectively. The cyclic shear strain is the strain amplitude that occurs during one cycle and the permanent shear strain is the strain that has increased from the initial time during repeated of N cycles.

Randolph et al. 2011 proposed a strain contour using cyclic simple shear test, and defined that number of failures is the number of times that permanent shear strain or double amplitude shear strain is equal to 15%, obtained from cyclic simple shear test results with asymmetric cyclic loading on normally consolidated Drammen clay. In this test, the permanent shear strain or double amplitude shear strain of 15% are defined as the failure criterion considering the conditions of offshore structures. The general design graph proposed by Andersen et al. 1999 was normalized to the effective stress, however, the modified design graph was normalized to the undrained shear strength considering the initial pore water pressure.

## 3 CYCLIC SIMPLE SHEAR TEST

### 3.1 *Principle of cyclic direct simple shear test*

In this study, the test was performed using a cyclic direct simple shear apparatus as shown in Figure 2 (a). Cyclic direct simple shear test can accurately measure dynamic characteristics with cyclic loading in a large to medium strain range. Cyclic direct simple shear test is performed by considering an earth pressure at rest ($K_0$) condition to the specimen and constraining the

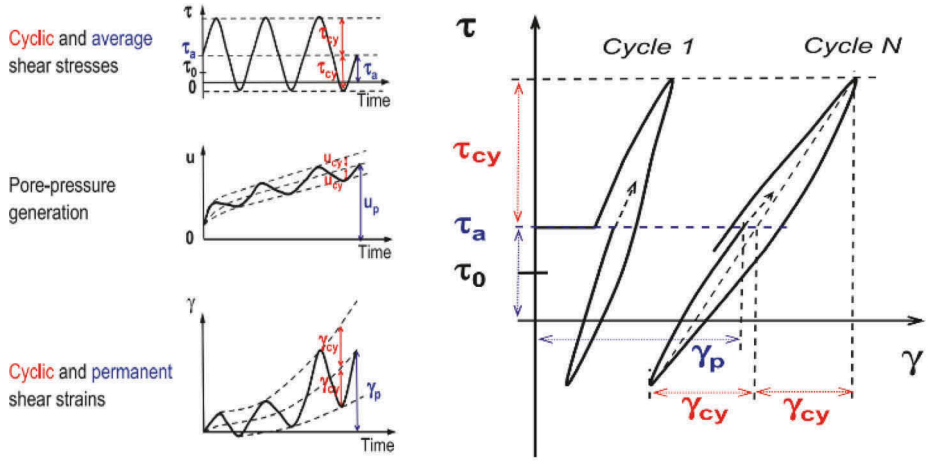


Figure 1. Pore-pressure and shear strain as function of time under un-drained cyclic loading, Andersen 2009. (a) Pore-pressure and shear strain as function of time under undrained cyclic loading. $u$, pore pressure; $\gamma$, shear strain; $\tau_0$, initial consolidation shear stress. (b) Stress-strain behaviour under cyclic loading.

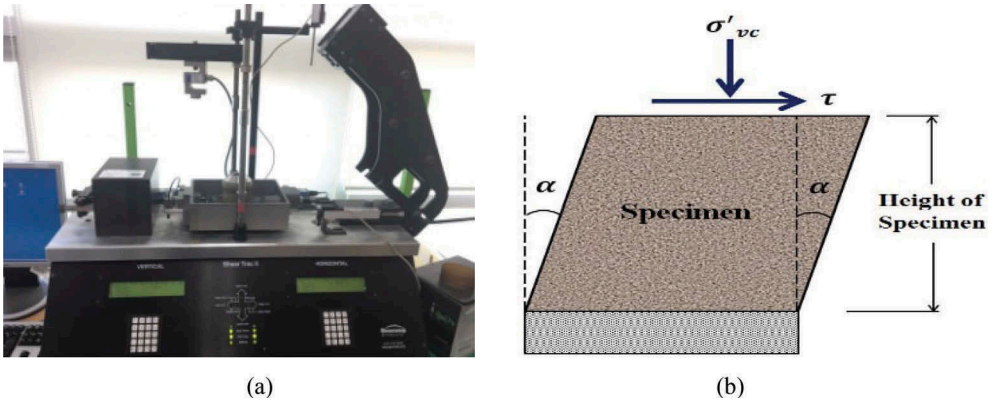


Figure 2. Test apparatus (a) Direct simple shear apparatus (b) Simple shear condition.

specimen with a wire reinforced membrane manufactured according to ASTM standard D6528-17 under such stress conditions. While shear stress is applied, height of specimen is controlled to maintain a constant volume, and it is assumed that changes of vertical stress is same as changes of pore pressure under undrained condition. Figure 2 (b) shows the principle of the direct simple shear test. The vertical stress is applied to the specimen while shear strain and shear stress is measured.

### 3.2 *Test conditions and setup*

The specimen used in the cyclic direct simple shear test was 63.5mm in diameter, and 21.5 to 23.4mm in height. The initial relative density was 50%. In this experiment, the applied frequency of 0.1Hz corresponding the wave loading period in the offshore structures was used. The failure criterion for the double amplitude of shear strain and permanent shear strain of 15% was employed. An additional failure criterion for the occurrence of liquefaction when the effective stress became zero was also used. The $K_0$ state was reproduced by constraining the lateral displacement with reinforced membrane, and the actual soil condition was implemented by applying the vertical consolidation stress before applying the shear stress. Vertical consolidation stress was set to 200-300 kPa within the expected stress range on the foundation of the offshore wind turbine generator.

This study used relatively uniform fine silty sand soils collected from the Saemangeum area near the west coast of Korea where offshore wind farms are planned to be constructed. To analyze the soil properties, specific gravity and grain-size analysis were performed. The maximum void ratio ($e_{max}$) and the minimum void ratio ($e_{min}$) were obtained using BS1377, JSF T161-1990. Table 1 shows the soil properties used in this experiment.

Sample preparation affects the behavior of sandy soil. In this study, samples were prepared by air pluviation method with dry tamping method. The dropped samples were divided into five layers to obtain the same density. The cyclic direct simple shear test apparatus used in this test has a system that controls the vertical stress and loading in real time in order to keep the volume constant during test process (undrained condition). Saturated undrained tests can be performed on dry samples based on the fact that the changes of vertical stress while the

Table 1. Properties of west coast marine silty sand.

| Max. voids ratio | Min. voids ratio | Uniformity coefficient | Coefficient of curvature | USCS | Specific gravity |
|---|---|---|---|---|---|
| 1.18 | 0.74 | 1.80 | 0.15 | SP-SM | 2.62 |

sample volume keeps constant is equal the changes of pore water pressure under undrained condition, Budhu & Britto 1987. Shear control in cyclic direct simple shear test can either be deformation control or stress control. The stress control refers to the conditions in which the shear stress under a constant rate applies to the soil specimen, so that actual loading conditions are simulated. In this study, the stress control method was used.

## 4 TEST RESULTS AND ANALYSIS

Static and dynamic tests were performed under various stress conditions, and the differences in stress behavior, shear stress, shear strain, and pore water pressure under various confining pressure were analyzed.

### 4.1 *Monotonic test and specimen condition*

Static tests were performed on the west coast silty sand with different confining pressures. Shear was applied at 0.3 mm/min. A same failure criterion of 15% shear strain was employed in three static tests. An effective internal friction angle of 29.9° was obtained (Figure 3) and static stress ratio was 0.574. This is the case where the cyclic shear stress ratio equals zero, and is defined as the starting point of the stress-based failure contour.

### 4.2 *Stress behavior*

In order to compare the behaviors at various conditions, cyclic direct simple shear tests were performed at various average shear stress ratio (0.1~0.5) and cyclic shear stress ratio (0.1~0.5). Figures 4 and 5 show the changes of shear stress, shear strain, and pore water pressure when the average shear stress ratio (ASR) is 0 and the cyclic shear stress ratio (CSR) is 0.3 under confining pressure of 200kPa and 300kPa, respectively. In the case of average shear stress ratio is zero, assuming that there is no shear stress from the self-weight of structure and in-situ. Figures 4 and 5 show the results in which the average shear stress ratio is zero. Although the confining pressure is different, the main deformation mode experienced symmetrical trend and permanent shear deformation occurred at a very small value. This result shows that as the number of cycles increases, only the shear strain increases. This is because the cyclic shear strain is occurred by cyclic shear stress, and permanent shear strain does not occur because the average shear stress does not act. In the Figure 4 when the confining pressure is 200kPa, pore water pressure increases before shear strain (permanent or average) reaches failure criterion of 15%, and failure occurred when the effective normal stress becomes zero at 12 cycles. On the other hand, in the Figure 5 when the confining pressure is 300kPa, the shear strain (permanent or average) reached failure criterion of 15% at 13 cycles. Under the same cyclic shear stress ratio (0.3) condition, however, it can be seen that the criterion governing the failure is depending on the confining pressure.

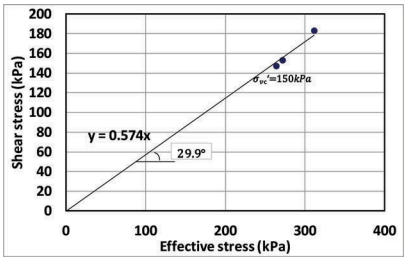


Figure 3. Effective internal friction angle.

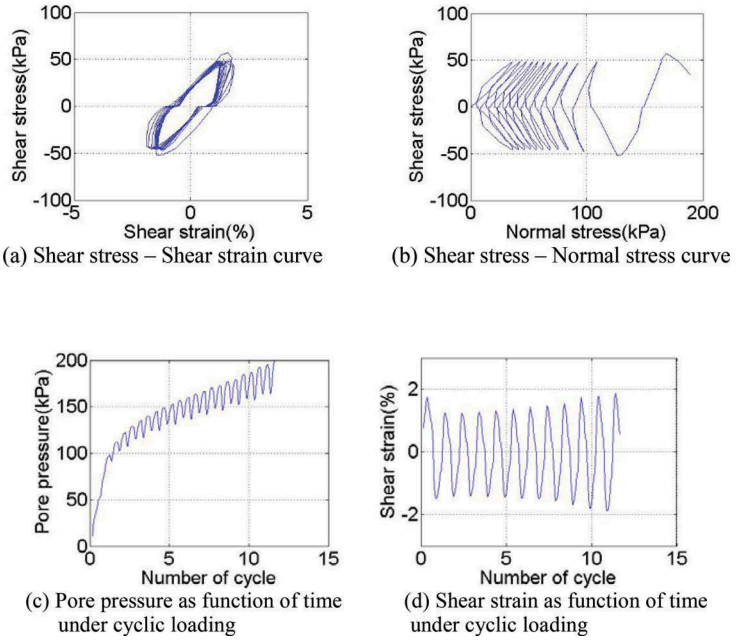


(a) Shear stress – Shear strain curve
(b) Shear stress – Normal stress curve
(c) Pore pressure as function of time under cyclic loading
(d) Shear strain as function of time under cyclic loading

Figure 4. Stress behavior (Confining pressure=200kPa, ASR=0, CSR=0.3, cycle=12), Son et al. 2017.

Figures 6 and 7 show the changes of shear stress, shear strain, and pore water pressure when the average shear stress ratio is 0.3 and the cyclic shear stress ratio is 0.3 at the confining pressure of 200kPa and 300kPa, respectively. According to Figures 6 (a) and 7 (a), when the average shear stress ratio is larger than 0, the permanent shear strain increases as the number of cycle increases, however, cyclic shear strain is constant. Figures 6 (a) and 7 (a) show the increase of permanent shear strain. Main deformation mode has same shape even though the confining pressures are different.

In Figure 6, under the same conditions of average shear stress ratio (0.3) and the cyclic shear stress ratio (0.3), in addition to the confining pressure of 200kPa, the shear strain (permanent or average) was reached the failure criterion of 15% at 10 cycles or more.

On the other hand, in Figure 7 with the confining pressure of 300kPa, the failure occurs at 3761 cycles. This result shows that even though the average shear stress ratio is greater than zero, application of high confining pressure results in significantly increases the number of cyclic loading reaching the failure criterion compared to lower level confining pressure, as the average shear stress ratio becomes zero. Furthermore, under confining pressure of 300kPa, the pore water pressure rapidly increases when the cyclic loading begins, and then experiences gradual increase, while under confining pressure of 200kPa it increases steadily without sudden change till reaching the failure (Figure 6 (c), Figure 7 (c)).

### 4.3 *Failure contour*

The failure contour shows curves that connect the same number of cycles reaching failure with respect to cyclic shear stress ratio and average shear stress ratio. The starting point of the failure lines (CSR=0) was obtained from the static test.

As shown in Figure 8, when the CSR or ASR value are constant and ASR or CSR increases, the number of cyclic loading reaching failure criterion decreases. The failure contour under the confining pressure of 200kPa tends to move downward compared to those of 300kPa. Failure at two cases, mainly occurs by cyclic shear strain (double amplitude shear strain of 15%) with the average shear stress ratio close to zero. When the average shear stress

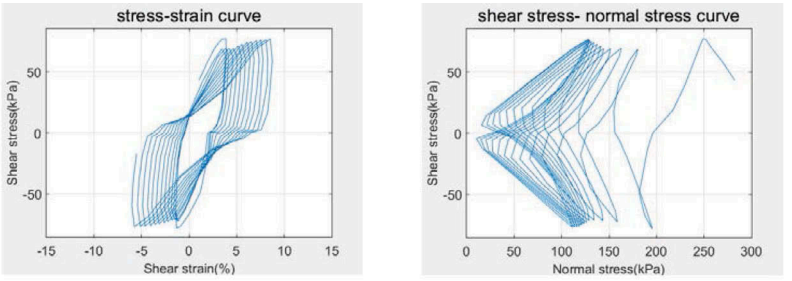


(a) Shear stress – Shear strain curve (b) Shear stress – Normal stress curve

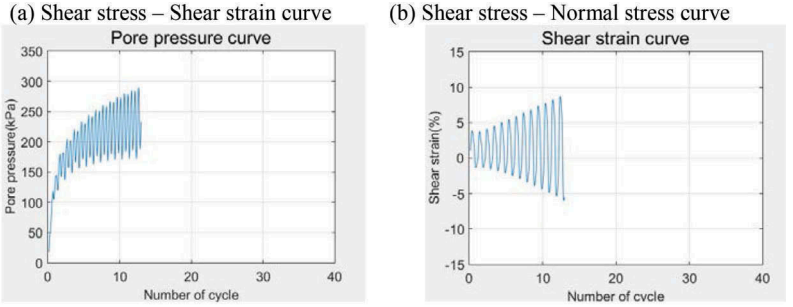


(c) Pore pressure as function of time under cyclic loading

(d) Shear strain as function of time under cyclic loading

Figure 5. Stress behavior (Confining pressure=300kPa, ASR=0, CSR=0.3, cycle=13).

ratio increases, the failure is occurred by permanent shear strain rather than cyclic shear strain. Failure contour in Figure 8 can be used as a useful design tool to determine the design conditions such as cyclic shear stress ratio, average shear stress ratio, number of cyclic loading corresponding to the confining pressure. The proposed failure contour shows that number of

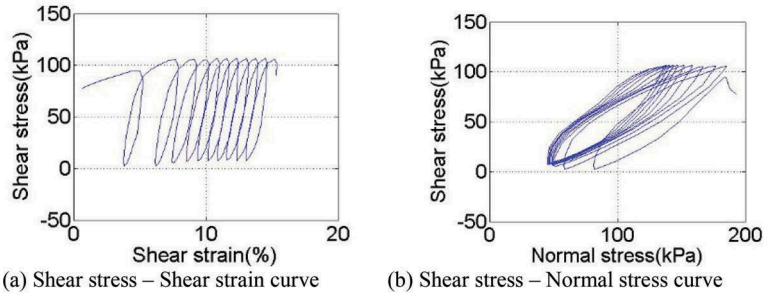


(a) Shear stress – Shear strain curve (b) Shear stress – Normal stress curve

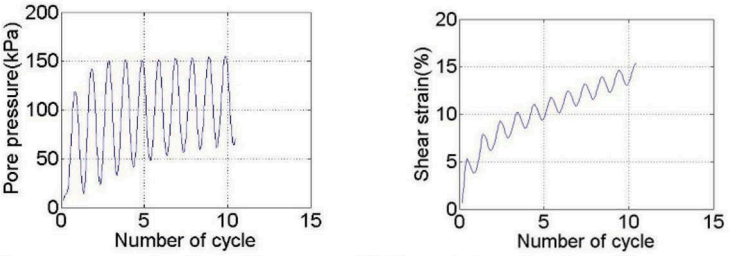


(c) Pore pressure as function of time under cyclic loading

(d) Shear strain as function of time under cyclic loading

Figure 6. Stress behavior (Confining pressure=200kPa, ASR=0.3, CSR=0.3, cycle=10), Son et al. 2017.

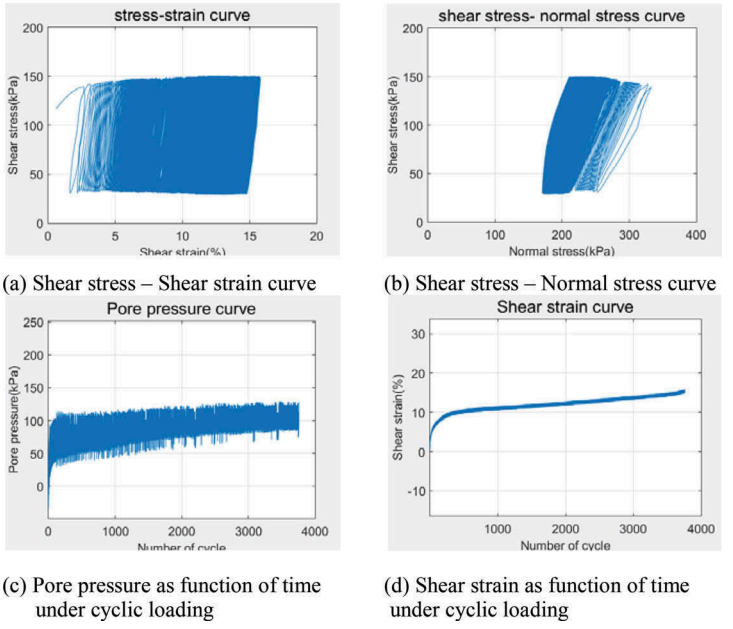


(a) Shear stress – Shear strain curve

(b) Shear stress – Normal stress curve

(c) Pore pressure as function of time under cyclic loading

(d) Shear strain as function of time under cyclic loading

Figure 7. Stress behavior (Confining pressure=300kPa, ASR=0.3, CSR=0.3, cycle=3761).

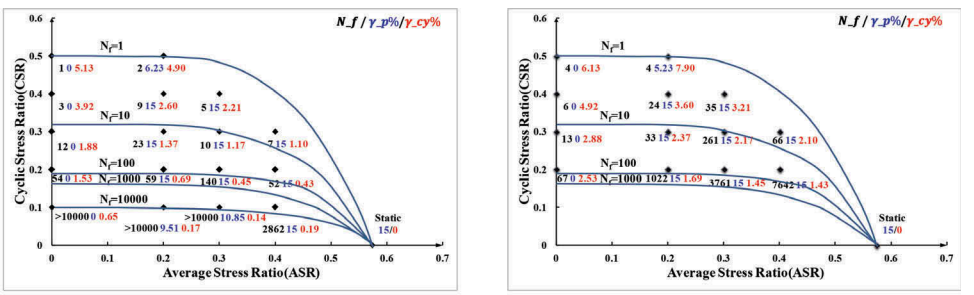


(a) Confining pressure=200kPa, Ko et al. 2017

(b) Confining pressure=300kPa, Yoon 2018

Figure 8. Failure contours for marine silty sand.

cyclic loading reaching failure is dependent on the cyclic shear stress ratio, confining pressure, and average shear stress ratio.

## 5 SUMMARY AND CONCLUSIONS

In order to evaluate the effect of average shear stress and cyclic shear stress on the undrained shear failure behavior at different confining pressures, several cyclic direct simple shear tests were performed on the west coast silty sand of Korea. The summary and conclusions are as follows.

1. When the average shear stress ratio is zero, although the confining pressure is different, the principal deformation mode experiences symmetrical trend and permanent shear deformation occurs at a very low value. This result shows that as the number of cycles increases,

only the shear strain is increased, this is because the cyclic shear strain is occurred by cyclic shear stress and permanent shear strain does not occur since the average shear stress does not act.
2. When the average shear stress ratio is greater than zero, application of high confining pressure significantly increases the number of cyclic loading reaching the failure criterion compared to lower level confining pressure, as the average shear stress ratio becomes zero. Furthermore, under confining pressure of 300kPa, the pore water pressure rapidly increases when the cyclic loading begins, and then experiences gradual increase, while under confining pressure of 200kPa it increases steadily without sudden change till reaching the failure.
3. Failure contour presented in this study can be used as a useful design tool to determine the design parameters such as cyclic shear stress ratio, average shear stress ratio, number of cyclic loading corresponding to the confining pressure.
4. The proposed failure contour shows that number of cyclic loading reaching failure is dependent on the cyclic shear stress ratio, confining pressure, and average shear stress ratio.

## ACKNOWLEDGEMENT

This paper was financially supported by the National Research Foundation of Korea (NRF-2017R1A2B4010201) and the Ministry of the Interior and Safety as Earthquake Disaster Prevention Human resource development Project.

## REFERENCES

Andersen, K.H. 2009. Bearing Capacity under Cyclic Loading - Offshore, Along the Coast and on Land. The 21st Bjerrum Lecture presented in Oslo, 23November 2007. NRC Research Press. Web site www.cgj.nrc.ca.

Andersen, K.H. & Berre, T. 1999. Behaviour of a Dense Sand under Monotonic and Cyclic Loading. In Proceedings of the 12th ECSMGE, *Geotechnical Engineering for Transportation Infrastructure, Amsterdam, the Netherlands, 7–10 June 1999*. 2: 667–676.

Andersen, K.H., Kleven, A., & Heien, D. 1988. Cyclic Soil Data for Design of Gravity Structures. *Journal of Geotechnical Engineering* 114(5): 517–539.

Budhu, M., and Britto, A. 1987. Numerical Analysis of Soils in Simple Shear Devices. *Soils and Foundation* 27(2): 31–41.

Ko, M.J., Son, S.W., Kim, J.M. 2017. Relative Density and Stress-Dependent Failure Criteria of Marine Silty Sand Subject to Cyclic Loading. *Journal of the Korean Geotechnical Society* 33(1): 79–91.

Miura, S. and Toki, S. 1982. A Sample Preparation Method and It Effect on Static and Cyclic Deformation-strength Properties of Sand. *Soils and Foundation* 22: 61–77.

Nielsen, S.D., Shajarati, A., Sorenson, K.W., and Ibsen, L.B. 2012. Behaviour of Dense Frederikshavn Sand during Cyclic Loading. *DCE Technical Memorandum* 15: 1–9.

Peck, R.B., Hanson, W.E., and Thornburn, T.H. 1974. *Foundation Engineering 2nd Edition*. New York: John Wiley and Sons.

Randolph, M. and Gourvenec, S. 2011. *Offshore Geotechnical Engineering*. Taylor and Francis, London.

Ryu, T.G. 2016. Long-term dynamic behavior study of marine silty sand for offshore structure foundation design. *Master's Thesis*, Pusan National University.

Ryu, T.G. and Kim, J.M. 2015. Stress-Dependent Failure Criteria for Marine Silty Sand Subject to Cyclic Loading. *Journal of the Korean Geotechnical Society* 31(11): 15–23.

Son, S.W., Ko, M.J., and Kim, J.M. 2017. Cyclic Shear Behavior Characteristics of the Marine Silty Sand. *Journal of Mechanical Science and Technology*-Taiwan 25(6): 784–790.

Vaid, Y.P. and Negussey, D. 1988. Preparation of Reconstituted Sand Specimens. *ASTM STP*, 977: 405–417.

Yoon, J.C. 2018. Evaluation of Ground Behavior due to Confining Pressure of Silty Sand in the West Sea. *Master's Thesis*. Pusan National University.